Exploration of complex multilayer film growth morphologies: STM analysis and predictive atomistic modeling for Ag on Ag(111)

Maozhi Li, P.-W. Chung, E. Cox, C. J. Jenks, P. A. Thiel, and J. W. Evans
Institute of Physical Research and Technology, Department of Chemistry, Department of Materials Science and Engineering, Department of Mathematics, and Ames Laboratory-U.S. DOE, Iowa State University, Ames, Iowa 50011, USA
(Received 12 October 2007; published 3 January 2008)

Scanning tunneling microscopy studies are integrated with development of a realistic atomistic model to both characterize and elucidate the complex mounded morphologies formed by deposition of Ag on Ag(111) at 150 and 180 K. Threefold symmetric lateral shapes of islands and mounds are shown to reflect the influence of a nonuniform step edge barrier inhibiting interlayer transport. Modeling of structure at the mound peaks leads to a sensitive estimate of the magnitude of this large barrier.

DOI: 10.1103/PhysRevB.77.033402 PACS number(s): 68.55.A−, 68.37.−d, 68.43.Jk

Deposition drives film growth far from equilibrium and can produce an extraordinary variety of complex film morphologies.[1] This is the case even for strain-free homoepitaxial growth. Limited edge diffusion generates irregular island shapes,[2] and inhibited interlayer transport due to the presence of an Ehrlich-Schwoebel (ES) step edge barrier produces mounds (multilayer stacks of two-dimensional islands). In the case of large ES barriers, these mounds can exhibit terraced wedding-cake-like structures reminiscent of highly eroded landscapes.[1] Encoded in these complex morphologies are details of the underlying atomistic processes controlling growth. Furthermore, the variation of morphology with surface temperature (T) reflects the associated energetics.

A key challenge is to extract information about such processes and energetics from suitable analysis. Simple analytic modeling may extract the terrace diffusion barrier from submonolayer island densities at low T and the magnitude of the ES barrier from the initial population of higher layers.[1] However, complete understanding of complex multilayer morphologies is most convincingly (but rarely) demonstrated by successful development of predictive atomistic lattice-gas models. These should be capable of describing the growth not just for a single T but for a range of T, potentially exhibiting quite different morphologies. Such model development integrated with scanning tunneling microscopy (STM) experiments might also reliably determine the rates or activation barriers for key surface diffusion processes.[3]

Homoepitaxial growth of Ag on Ag(111) is a "classic" system which provides a prototype for rapid kinetic roughening involving formation of mounded morphologies and which also exhibits dramatic island shape transitions. However, there are still basic unresolved issues for this growth system, so it is chosen here as a case study. Previous transmission electron microscopy[4] and STM studies[5] have revealed wedding-cake-like mounds for growth at 300 K. However, their lateral sizes at 300 K were so large due to rapid terrace diffusion that these morphologies were impacted by substrate dislocations. Other studies of this system were directed toward determination of the ES barrier, still a subject of much controversy.[6] These included analyses of island decay, initial population of higher layers,[6] and also diffraction studies of multilayer growth and kinetic roughening for various T below 300 K.[7–9] The latter indicated so-called Poisson growth reflecting negligible interlayer transport due to an effectively insurmountable ES barrier: the surface roughness defined as the rms variation of film height (in units of interlayer spacing) satisfies $W \approx \theta^{1/2}$ for coverage θ in monolayers (MLs). The W values smaller than $\theta^{1/2}$ reflect downward transport, and larger values can only be achieved with upward transport between layers. Surprisingly, for Ag/Ag(111), there has been no systematic real-space STM investigation of multilayer growth morphologies for lower T between 100 and 200 K where expected dramatic changes in island and mound structures are not readily assessed from more limited diffraction data.

In this Brief Report, we present a comprehensive analysis combining both STM and realistic atomistic modeling for multilayer growth of Ag on Ag(111) focusing on deposition at 150 and 180 K. Kinetic Monte Carlo (KMC) simulation of island shape behavior under judiciously selected conditions unequivocally reveals the existence and impact of a nonuniform ES barrier. This conclusion is supported by analysis of energetics using semiempirical potentials. We find that complex transitions in submonolayer island shapes between 120 and 200 K are propagated into lateral shapes of multilayer mounds and that growth is Poisson-like. Our multilayer analysis focuses on the mean size of top layers of mounds which, in contrast to surface roughness W, is shown to be highly sensitive to magnitude of the ES barrier. The goal of reliable model prediction of diverse growth behavior for different T is achieved, but it requires also accounting for the onset of reversibility in island formation in this T regime.

Our experimental procedures are described in Ref. 10. (ultra high vacuum system with base pressure $\sim 1 \times 10^{-10}$ Torr; Ag(111) sample from Princeton scientific cooled with liquid nitrogen; deposition using an Omicron EFM3 evaporator with Ag flux of 0.003 ML/s; imaging of the film morphology using an Omicron VTSTM.) Growth of Ag films on Ag(111) up to ~3–5 ML was monitored between 120 and 200 K. Our atomistic lattice-gas model incorporates the appropriate fcc(111) crystal structure where steps have distinct A- and B-type structures for orientations differing by 60°.[1,10] Deposition at rate 0.003 ML/s accounts for downward funneling of atoms deposited right at step edges (although this process has minimal effect for morphologies

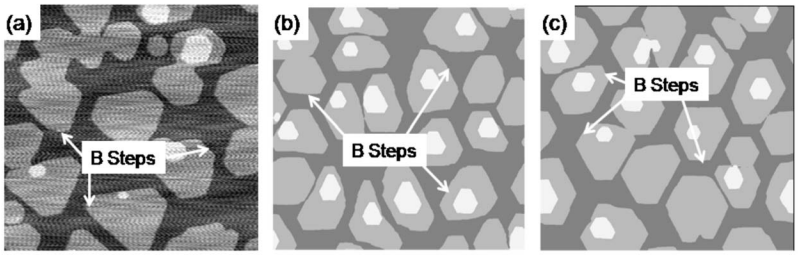

FIG. 1. Ag islands on Ag(111) for 0.7 ML at 180 K. (a) STM image. KMC simulation with (b) uniform ES barrier of 0.1 eV and (c) nonuniform ES barrier (0.08 eV at B steps; 0.16 eV at A steps). Image sizes: $\sim 280 \times 280$ nm^2. The B-step orientation is maintained in Figs. 2 and 4.

considered here with broad terraces). Adatoms reside at threefold hollow fcc sites in each layer and can only hop between fcc sites. We choose a common prefactor of 10^{11}/s for both intra- and interlayer diffusions of isolated atoms and a terrace diffusion barrier of 97 meV as determined previously.[1] The ES barriers at portions of steps with local A-type and B-type orientations are treated as distinct free parameters. Edge diffusion parameters were chosen to recover submonolayer island shapes described below.[10,11] The system size in our KMC simulations is $\sim 280 \times 280$ nm^2.

Inhibited edge diffusion produces the following complex shape transitions of Ag islands on Ag(111) as observed at $\sim$0.3 ML:[10] dendritic shapes with triangular envelopes at $\sim$120 K; fairly isotropic "fat fractals" at $\sim$150 K; and distorted hexagons at $\sim$180 K. The equilibrium island shapes are near-perfect hexagons due to almost equal A- and B-step energies,[12] so the shape deviations from sixfold symmetry are purely kinetic in origin. The following observations are of key relevance for our study. At $\sim$120 K, atoms aggregating with single atoms attached to straight edges can relax to kink sites much more easily at B steps than at A steps. Thus, growth orthogonal to A steps is faster, producing the dendrites with triangular envelops aligned with B steps. This so-called "anisotropy in corner rounding (ACR)"[13] also ensures that atoms aggregating at corners of distorted hexagonal islands at 180 K more easily reach A steps than B steps.[10] Consequently, growth controlled by ACR produces shorter A steps and longer B steps.

However, STM studies of deposition at 180 K with a judiciously selected higher coverage of 0.7 ML instead find distorted hexagonal island shapes with shorter B steps and longer A steps [see Fig. 1(a)].[14] To elucidate this observation, we simulate island growth first selecting a uniform ES barrier so atoms descend at A and B steps with equal probability, and interlayer transport does not tend to distort hexagonal island shapes [see Fig. 1(b)]. Thus, the effect of ACR prevails to produce shorter A steps, inconsistent with experiment. Then, we introduce a nonuniform ES barrier, atoms descending more easily at B steps than at A steps. Our simulations show that for coverages below $\sim$0.5 ML, islands are distorted hexagons with shorter A steps. However, at higher coverages, more atoms deposit on top of islands, and their shapes evolve from having shorter A steps to having shorter B steps. Figure 1(c) shows the simulated morphology at 0.7 ML with nonuniform ES barrier. Easier descent of atoms at B steps causes these steps to grow out faster, overwhelming the effect of ACR and producing longer A steps [Fig. 1(c)], consistent with experiment.

Our demonstration of a nonuniform ES barrier is consistent with semiempirical embedded atom method (EAM) analysis of the interlayer transport energies. EAM is not expected to predict precise values of diffusion barriers, but it generally does correctly illustrate trends. Specifically, the EAM barriers for interlayer transport at portions of steps with local B-like structure (e.g., straight B steps or kinks on A steps) are similar and are about 1/2 of those for local A-like structure (e.g., straight A steps or kinks on B steps). This reflects the feature that exchange diffusion is facile for the former but not for the latter. Thus, in contrast to common perception, kinks do not always enhance downward transport: for Ag on Ag(111), downward transport is more facile at straight B steps than at kinks on those steps.[15] In our subsequent modeling, the ES barrier depends on the local step structure with a fixed ratio of 1/2 for B-like versus A-like structure, its magnitude being a free parameter.

Next, we turn to the analysis of complex multilayer growth morphologies for 3 ML films. Figure 2(a) shows the fat fractal mounds grown at 150 K, and Fig. 2(d) shows more regular shaped mounds grown at 180 K. In both cases, $W \sim \theta^{1/2}$ follows Poisson-like growth. This motivates running benchmark simulations of our atomistic model with an infinite ES barrier, which indeed produces morphologies with lateral shapes similar to experiment [Figs. 1(c) and 1(f)].[16] However, the islands or terraces forming the peaks of the mounds are much smaller than in experiment, and the side profiles of mounds are more sharply peaked. This can be understood from general considerations:[1] the ES barrier is large but not infinite; it does cause atoms landing on terraces on the sides of mounds to attach to ascending steps rather than to descend; but those landing on top cannot reach an ascending step, so interrogate the descending step many times, and are likely to descend; this enhances growth of the top layer islands. Thus, the mean size of these islands, in contrast to W, should be sensitive to the ES barrier magnitude. Simple estimates for this size have been developed assuming circular islands and a uniform ES barrier.[1] However, these treatments are not readily adapted to irregular mound shapes and nonuniform ES barriers.

Fortunately, application of our atomistic lattice-gas model allows direct assessment of relevant behavior. Simulations reveal a very rapid variation of the mean size of the top layer islands with the magnitude of the ES barrier (see below) potentially allowing effective determination of this magnitude by comparison with the experimental mean size. However, to be deemed reliable and predictive, the model should be able to reproduce the mean size of top layer islands measured in experiments at different T with the *same* choice of ES barrier. One complication is that the top layer size is determined not only by the ES barrier but also by the details of the nucleation process. Therefore, we first perform simu-

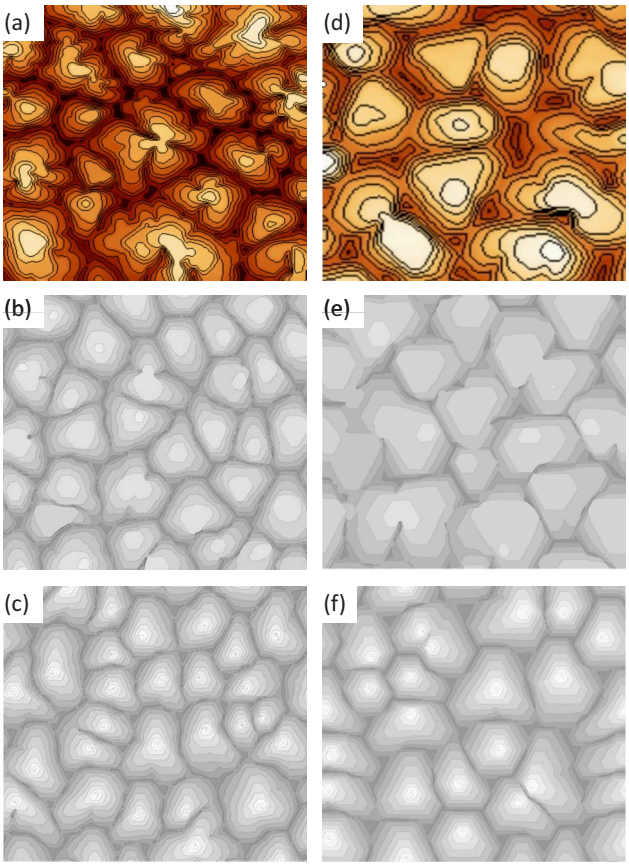

FIG. 2. (Color online) Comparison of 3 ML film morphologies of Ag/Ag(111) obtained from [(a) and (d)] STM and [(b), (c), (e), and (f)] KMC at [(a)–(c)] 150 K and [(d)–(f)] 180 K with [(b) and (e)] finite nonuniform and [(c) and (f)] infinite ES barriers, respectively. Images sizes: 175×175 nm^2 for 150 K and 280×280 nm^2 for 180 K.

lations of our atomistic model with reversible island formation allowing dimer dissociation controlled by a bond energy of 0.24 eV, but with stable trimers (i.e., a critical size of $i=2$). The bond energy is taken from previous density functional theory (DFT) analysis.[17] However, we find that the magnitude of the ES barrier must be chosen at least 30% lower at 180 K than at 150 K to match experiment. This indicates that the bond energy of 0.24 eV is higher than the physical value, making nucleation on top of islands too easy at 180 K (although still more difficult that at 150 K).

To resolve this inconsistency, we found that by selecting a lower Ag dimer bond energy of 0.18 eV, our modeling does produce a T-independent estimate of the ES barrier magnitude. In this case, island nucleation is highly reversible at 180 K (but still with $i=2$) and somewhat reversible at 150 K. Is this estimate of the bond energy realistic? Our recent extensive plane-wave DFT studies indicate that this bond energy converges unusually slowly with the size of the lateral unit cell used in the calculations. The previous high value of $\sim$0.24 eV came from a typical 4×4 choice,[17] but lower converged values of $\sim$0.19 eV are achieved with a 6×6 cell.[18]

The key analysis of the variation of top layer size with ES barrier is shown in Fig. 3. By comparing simulation predic-

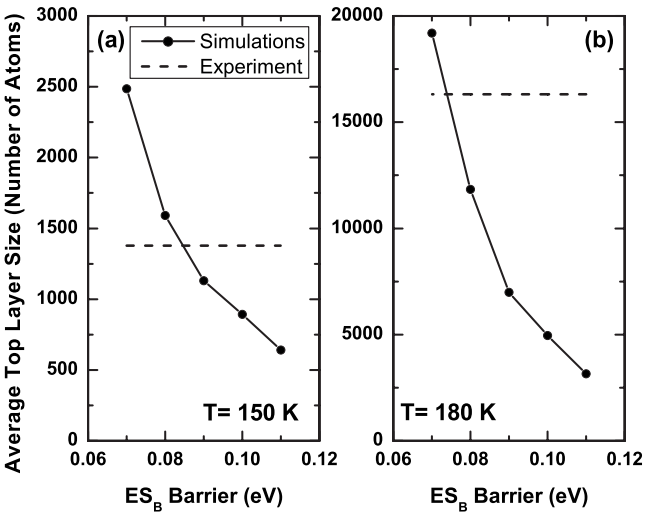

FIG. 3. Dependence of mean top layer island size for 3 ML films on the magnitude of the ES barrier at B steps (1/2 of the ES barrier at A steps): (a) 150 K and (b) 180 K.

tions with experimental values (horizontal dashed lines), we estimate an ES barrier of 0.085 eV for B steps by matching 150 K data [Fig. 3(a)], and a fairly consistent value of 0.075 eV by matching 180 K data [Fig. 3(b)], with double those values of 0.15–0.17 eV for A steps. These values are based on use of a common prefactor for intra- and interlayer diffusions. They should be compared with the commonly adopted effective or average value for the ES barrier of $\sim$0.13 eV (Ref. 6) with the ratio of interlayer to intralayer prefactors of either close to or above unity. However, reanalysis of those earlier studies is called for given our demonstration and characterization of nonuniformity in the ES barrier.

To gauge the challenge and success of our modeling, it should be noted that the experimental values for the mean top layer island size (which we match) differ by more than an order of magnitude between 150 and 180 K. Simulated images of the morphologies of 3 ML films in Fig. 2(b) at 150 K and Fig. 2(e) for 180 K capture all the features of the STM images in Figs. 2(a) and 2(b): our model matches not just only the lateral shapes and structure near the peaks of the mounds but also the average densities or lateral sizes of the mounds.

Having developed a predictive atomistic model, it can be used to explore complex morphological evolution for extended film growth to higher coverages or for different T. Figure 4 shows the predictions for film growth up to 20 ML at 150 K. The irregular fat fractal structure of submonolayer islands[10] is replaced by more compact but still irregular mound shapes. Subsequent shapes are controlled in part by packing of mound bases to cover the substrate. Reduction of the terrace widths during growth is enforced by the Poisson-like increase in roughness and the near absence of mound coarsening. There have been extensive attempts to quantify such features from diffuse diffraction profile data, particularly the mean and standard deviation of the terrace width distribution (both proposed to scale like $\sim\theta^{-2/3}$ at lower T).[9] However, those analyses were based on quasi-one-

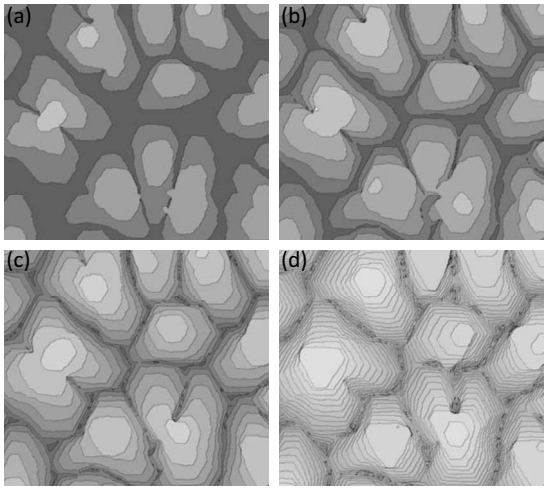

FIG. 4. Simulated morphologies at 150 K: (a) 1 ML, (b) 2 ML, (c) 4 ML, and (d) 20 ML. Images sizes: 100×100 nm^2.

dimensional Markovian models for film morphologies with assumed Γ distribution of terrace widths or on heuristic forms for oscillating height correlation functions. Direct analysis of our extended simulations as shown in Fig. 4, indicates a slower decrease in mean terrace width closer to $\sim\theta^{-1/2}$. In addition, previous studies of diffraction profiles at higher T indicated triangular symmetry with a preponderance of (111) facets associated with A steps rather than (100) facets associated with B steps.[8] This feature is apparent at 180 K in our STM images [Fig. 2(d)]. It is recovered in simulations with a nonuniform ES barrier [Fig. 2(e)] but not with a uniform or infinite ES barrier.

Despite long standing interest in the Ag/Ag(111) system as a prototype for rough multilayer growth, no comprehensive STM studies or realistic atomistic modeling were available and uncertainty persisted regarding interlayer transport. Here, we integrate STM studies with successful development of a predictive model for complex growth morphologies between 120 and 200 K. Description of growth must account for the onset of reversibility in island nucleation, complex transitions in island growth shapes, and a nonuniform ES barrier as demonstrated in this study.

This work was supported by NSF Grant No. CHE-0414376 and performed at Ames Laboratory-U.S. DOE (operated under Contract No. DE-AC02-07CH11358). M. L. was also supported by NSF of China (10704088). We thank C. Ghosh for EAM analysis.

[1] T. Michely and J. Krug, *Islands, Mounds, and Atoms* (Springer, Berlin, 2004); J. W. Evans, P. A. Thiel, and M. C. Bartelt, Surf. Sci. Rep. **61**, 1 (2006).
[2] R. Q. Hwang and M. C. Bartelt, Chem. Rev. (Washington, D.C.) **97**, 1063 (1997).
[3] K. J. Caspersen, A. R. Layson, C. R. Stoldt, V. Fournee, P. A. Thiel, and J. W. Evans, Phys. Rev. B **65**, 193407 (2002).
[4] K. Meinel, M. Klaua, and H. Bethge, J. Cryst. Growth **89**, 447 (1988).
[5] J. Vrijmoeth, H. A. van der Vegt, J. A. Meyer, E. Vlieg, and R. J. Behm, Phys. Rev. Lett. **72**, 3843 (1994).
[6] K. Bromann, H. Brune, H. Roder, and K. Kern, Phys. Rev. Lett. **75**, 677 (1995); K. Morgenstern, G. Rosenfeld, E. Laegsgaard, F. Besenbacher, and G. Comsa, *ibid.* **80**, 556 (1998); K. R. Roos and M. C. Tringides, *ibid.* **85**, 1480 (2000); **87**, 149602 (2001); J. Krug, *ibid.* **87**, 149601 (2001); K. Morgenstern and F. Besenbacher, *ibid.* **87**, 149603 (2001); J. Krug, P. Politi, and T. Michely, Phys. Rev. B **61**, 14037 (2000); Z. Chvoj and M. C. Tringides, *ibid.* **66**, 035419 (2002).
[7] W. C. Elliot, P. F. Miceli, T. Tse, and P. W. Stephens, Phys. Rev. B **54**, 17938 (1996).
[8] Ch. Ammer, T. Schaefer, Ch. Teichert, K. Meinel, and M. Klaua, Surf. Sci. **307-309**, 570 (1994).
[9] E. Z. Luo, J. Wollschlager, F. Wegner, and M. Henzler, Appl. Phys. A: Mater. Sci. Process. **60**, 19 (1995); J. Wollschlager, E. Z. Luo, and M. Henzler, Phys. Rev. B **57**, 15541 (1998); G. Rosenfeld, R. Servaty, C. Teichert, B. Poelsema, and G. Comsa, Phys. Rev. Lett. **71**, 895 (1993).
[10] E. Cox, M. Li, P. W. Chung, C. Ghosh, T. S. Rahman, C. J. Jenks, J. W. Evans, and P. A. Thiel, Phys. Rev. B **71**, 115414 (2005).
[11] Edge diffusion barriers were slightly modified from Ref. 10 to better describe observed island shapes: 0.28 (0.30 eV) along straight A (B) steps; 0.28 (0.33) eV from A (B) steps to corners; 0.08 (0.13) eV from corners to A (B) steps; prefactor of 10^{13}/s.
[12] C. Steimer, M. Giesen, L. Verheij, and H. Ibach, Phys. Rev. B **64**, 085416 (2001).
[13] H. Brune, H. Röder, K. Bromann, K. Kern, J. Jacobsen, P. Stoltze, K. Jacobsen, and J. Nørskov, Surf. Sci. **349**, L115 (1996).
[14] Longer B steps at high T were incorrectly reported in Ref. 10. The substrate used there at high T was reoriented by $\sim 180°$ from that used at low T (cf. Fig. 1).
[15] In contrast, on fcc(100) surfaces, kinks always facilitate downward transport via exchange which is aided by rapid edge diffusion. EAM indicates that downward transport on Ag(111) occurs via exchange at steps with local B-like structure (but not local A-like structure).
[16] At 180 K, these simulations actually invert the experimental triangular symmetry as explained below.
[17] K. A. Fichthorn and M. Scheffler, Phys. Rev. Lett. **84**, 5371 (2000).
[18] M. Shen, J. M. Wen, C. J. Jenks, P. A. Thiel, D. J. Liu, and J. W. Evans, Phys. Rev. B **75**, 245409 (2007).